layers we achieved were very compact films, i.e. the grains were densely arranged with a large number of inter-grain contacts. Moreover, the electrical measurements showed that Nb addition only had a negligible influence on the intergrain barrier. For these two reasons, magnification of surface effects for gas sensing may reasonably be expected to be bound up with the surface-to-volume ratio of the grains in the films, i.e. with the average size of the grains. Indeed, it is clear from the table that the smaller the grain size, the more sensitive the films. However, in order to achieve a quantitative relationship, further work needs to be done which takes into account the details of CO adsorption at the surface.

Finally, by comparing the measurements of Nb-doped TiO_2 samples annealed at 650 °C (anatase) to the ones at 850 °C (rutile), the measured response of the sensors exhibited no significant dependence on the structure of the lattice.

This work has demonstrated a way to produce nanosized TiO_2 films through the thick-film technique, a method which could be applied to extensive and low-cost production.

On the basis of the experience we have gained whilst carrying out these experiments, we conclude that preparation of stable nanostructured thick films of titania can be reproducibly achieved. We attribute such a performance to numerically controlled screen printing, for which accurate control of empirical parameters is possible.

Control of grain size was achieved by varying temperature and/or dopant addition. Also highlighted here is the way a nanophase magnifies the property of a material through the practical example of gas sensing.

The performance as a sensing layer is interesting because of the high degree of reproducibility by which the sensors can be produced and the negligible influence from humidity in CO detection. Qualitative agreement between structural features and electrical response was also inferred.

Received: October 20, 1998
Final version: May 5, 1999

[1] H. Tang, K. Prasad, R. Sanjinés, F. Lévy, *Sens. Actuators B* **1995**, *26–27*, 71.
[2] K. Bange, C. R. Ottermann, O. Anderson, U. Jeschkowsky, M. Laube, R. Feile, *Thin Solid Films* **1991**, *197*, 279.
[3] a) B. ORegan, M. Grätzel, *Nature* **1991**, *353*, 737. b) T. Gerfin, M. Grätzel, L. Walder, *Prog. Inorg. Chem*. **1997**, *44*, 345.
[4] X. Marguetettaz, D. Fitzmaurice, *J. Am. Chem. Soc.* **1994**, *116*, 5017.
[5] K. Sunada, Y. Kikuchi, K. Hashimoto, A. Fujishima, *Environ. Sci. Technol.* **1998**, *32*, 726.
[6] For a complete view of this topic see: *Proc. 1st Int. Conf. on Photocathodic Purification and Treatment of Water and Air* (Eds: D. F. Ollis, H. Al-Ekabi), Elsevier, New York **1993**.
[7] S. Y. Huang, L. Kavan, I. Exnar, M. Grätzel, *J. Electrochem. Soc.* **1997**, *142*, L142.
[8] M. Ferroni, V. Guidi, G. Martinelli, P. Nelli, G. Sberveglieri *Sens. Actuators B* **1997**, *44*, 499.
[9] G. Sberveglieri, L. E. Depero, M. Ferroni, V. Guidi, G. Martinelli, P. Nelli, C. Perego, L. Sangaletti, *Adv. Mater.* **1996**, *8*, 334.
[10] A. R. Bally, E. N. Korobeinikova, P. E. Schmid, F. Lévy, F. Bussy, *J. Phys. D, Appl. Phys.* **1998**, *31*, 1149.
[11] M. Ferroni, G. Faglia, V. Guidi, P. Nelli, G. Martinelli, G. Sberveglieri *Nanostruct. Mater.* **1996**, *7*, 709.
[12] L. E. Depero, L. Sangaletti, E. Bontempi, R. Salari, M. Zocchi, M. C. Casale, *J. Mater. Res.* **1998**, *13*, 1644.
[13] M. Musci, M. Notaro, F. Curcio, M. C. Casale, G. De Michele, *J. Mater. Res.* **1992**, *7*, 2846.
[14] H. Tang, K. Prasad, R. Sanjinès, P. E. Schmid, F. Lévy, *J. Appl. Phys.* **1994**, *75*, 2042.
[15] D. C. Hague, M. J. Mayo, *Nanostruct. Mater.* **1993**, *3*, 61.
[16] H. Hahn, *Nanostruct. Mater.* **1993**, *2*, 251.
[17] F. Bregnani, C. Casale, L. E. Depero, I. Natali-Sora, D. Robba, L. Sangaletti, G. P. Toledo, *Sens. Actuators B* **1996**, *31*, 25.
[18] U. Kirner, K. D. Schierbaum, W. Göpel, B. Leibold, N. Nicoloso, W. Weppner, D. Fischer, W. F. Chu, *Sens. Actuators B* **1990**, *1*, 103.
[19] P. K. Clifford, D. T. Tuma, *Sens. Actuators* **1982**, *3*, 255.
[20] V. Lantto, P. Romppainen, S. Leppävuori, *Sens. Actuators* **1998**, *14*, 149.
[21] M. C. Carotta, C. Dallara, G. Martinelli, L. Passari, A. Camanzi, *Sens. Actuators B* **1991**, *3*, 191.
[22] M. C. Carotta, M. Ferroni, D. Gnani, V. Guidi, M. Merli, G. Martinelli, M. C. Casale, M. Notaro, *Sens. Actuators B*, in press.
[23] N. Yamazoe, N. Miura, in *Some Basic Aspects of Semiconductor Gas Sensors in Chemical Sensor Technology*, Vol. 4 (Ed: S. Yamauchi), Kodansha, Tokyo, Elsevier, Amsterdam **1992**, p. 19.

Large-Area Patterning by Vacuum-Assisted Micromolding**

By *Noo Li Jeon*, *Insung S. Choi*, *Bing Xu*, and *George M. Whitesides**

This paper describes a procedure that allows rapid micropatterning of polymers over rigid and flexible substrates. This procedure utilizes a variation of micromolding in capillaries (MIMIC)[1–4]—vacuum-assisted MIMIC—to achieve rapid filling of capillaries. The approach is compatible with a broad range of materials, and is capable of generating features as small as 25 μm over a 3 inch wafer in less than 15 s (complete filling of the capillaries takes 15 s for 25 μm (width) × 50 μm (height) channels, and larger features take shorter times). We illustrate the utility of the technique by additive patterning of polypyrrole over a flexible 3 in. × 3 in. polyimide sheet.

Recent research in organic conductors and semiconductors has been motivated, in part, by the possibility of fabricating low-cost, large-area, flexible electronic[5,6] and optoelectronic[7,8] devices from these organic materials. Although appropriate materials have been developed for many types of devices, including organic transistors,[9–12] organic light-emitting diodes (LEDs),[13–15] and others, patterning these materials has been difficult using standard photolithography, lift-off, and etching. We wished to find processes for patterning electrically conductive polymers (and other functional organic materials) that would simplify fabrication and reduce costs.

[*] Prof. G. M. Whitesides, Dr. N. L. Jeon, I. S. Choi, Dr. B. Xu
Department of Chemistry and Chemical Biology
Harvard University
12 Oxford Street, Cambridge, MA 02138 (USA)

[**] This work was supported by the Defense Advanced Research Project Agency/SPAWAR and DARPA/AFRL. It used MRSEC Shared Facilities supported by the National Science Foundation (DMR-9400396).

  0935-9648/99/1108-0946 $ 17.50+.50/0

ADVANCED MATERIALS

Functional transistors have been fabricated in polymers by screen printing,[16] but the performance and size of these devices were limited by the modest resolution of the screen printing method (~100 μm). Recently, screen printing was combined with MIMIC to fabricate organic microelectronic devices.[17] In that work, components with large feature sizes (dielectrics) were defined by screen printing and fine features (electrodes, <100 μm) were patterned by MIMIC, albeit over a relatively small area.

Several approaches to patterning conducting organic polymers[6,17,18] and electroluminescent polymers[19,20] have been demonstrated and proposed. For example, conducting films of polyaniline have been patterned photochemically by using exposure to light to convert them from the conducting to the non-conducting form;[6] this process generated conducting tracks embedded in an insulating matrix. Rogers et al. have patterned a film of poly(*p*-phenylenevinylene) (PPV)[19] precursor by solvent-assisted micromolding[21] to fabricate polymer light-emitting devices that produced patterns of light localized to submicrometer areas. An elastomeric membrane has also been used as dry lift-off masks for patterning electroluminescent materials (TPD (*N,N′*-diphenyl-*N,N′*-bis(3-methylphenyl)-1,1′-biphenyl-4,4′-diamine) and tris(8-hydroxyquinoline) aluminum (Alq_3)).[20]

We have developed MIMIC in order to generate microstructures of a variety of materials[1,2] with feature sizes from one to several hundred micrometers and have begun to define its potential by the fabrication of multi-level electronic devices (Si MOSFETs (metal oxide semiconductor field effect transistors),[22] GaAs high electron mobility transistors (HEMTs),[23] diodes,[24] and rectifiers[25]). Two characteristics of MIMIC that have hindered its use in applications involving patterning over large areas are: i) polymers fill the channels slowly by capillarity, and, as a result, ii) it has been difficult to fill large areas with fine features.

The work reported here focuses on rapid patterning of large areas by MIMIC by accelerating the flow of polymer in the channels using low vacuum. We used vacuum-assisted MIMIC with a multi-point inlet scheme to pattern 25–100 μm features in polymer (Fig. 1). Using this process, it is possible to pattern a 3 inch wafer in less than 15 s (15 s is the time required to fill the channels with polymers; additional time is needed to cure the polymer with UV or heat). The mold used was made of a thin (200 μm) polydimethylsiloxane (PDMS) membrane attached to a rigid plate of glass or surface-oxidized polystyrene. This backing plate had holes drilled through it to introduce the prepolymer (outer holes) and to connect to vacuum (inner holes). Although this plate both supported the thin embossed PDMS mold and minimized distortions in the pattern,[26] vacuum-assisted MIMIC worked only for channels higher than 5 μm: smaller channels often failed, probably as a result of collapse of the channel under vacuum.

The procedure for vacuum-assisted MIMIC is similar to that already described for MIMIC.[1,2] The mold, membrane gasket, and the top plate were placed on the substrate and then

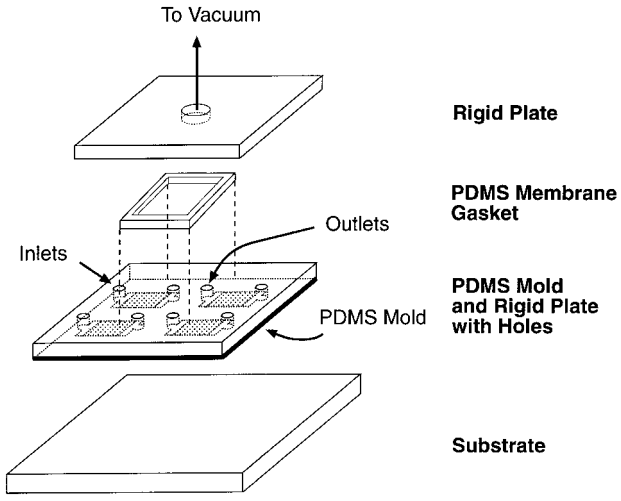

Fig. 1. Schematic illustration of the setup used in vacuum-assisted MIMIC with multi-point inlet design. Prepolymer was applied at the outer holes and the vacuum was applied at a single point near the center. The multi-point inlet design combined with vacuum-assisted MIMIC allowed rapid filling of capillaries over a large area.

the assembly was connected to the vacuum line (10 torr). The valve to vacuum was closed while the prepolymer was applied at the several outer entry points on the substrate. Since the thin PDMS gasket enclosed all of the inner holes, it was sufficient to apply the vacuum to a single point at the center of the substrate. This arrangement facilitated simultaneous filling of the capillaries over the entire area of the substrate. After the capillaries had been filled, the vacuum was released, the liquid prepolymer was converted to solid by UV irradiation, and the mold was removed to leave the patterned polymer.

The use of vacuum in filling the capillaries is attractive for two reasons. First, rapid filling of long capillaries is practical (5 cm in less than a minute). Filling long capillaries with similar dimensions by capillarity alone takes longer than 10 min and often results in incomplete filling. Second, the formation of thin underlayers in the areas where the PDMS mold touches the substrate can be avoided, because the mold and the substrate are in tight contact when vacuum is applied. The probability of forming an underlayer by capillary wicking between the substrate and the mold is further reduced by the short times required for filling. The elimination of this underlayer is important, since its presence may require an additional process step such as plasma etching or reactive ion etching (RIE) to remove it.

The time it takes to fill a channel of given dimensions with a liquid by capillarity depends on the inverse of the drop in the pressure between the start and end of the capillary.[27] To reduce the capillary filling time, while keeping the channel dimensions and the viscosity of the liquid constant, it is necessary to increase the pressure difference. We chose vacuum instead of pressure to generate this pressure differential since it is easier to maintain the seal between the mold and the substrate required by MIMIC when the channels are under negative pressure than under positive pressure.

  0935-9648/99/1108-0947 $ 17.50+.50/0

We have used MIMIC to form patterned polymeric structures on a variety of substrates, including Si/SiO_2, glass, and polymeric films (for example, polyimide and poly(ethylene terephthalate) (PET)). Figure 2A shows a partially patterned 3 inch Si wafer after 10 min of MIMIC without vacuum using a UV-curable polyurethane (NOA 73, Norland Optical, NJ) with viscosity of ~100 cPs (100 $kg\,m^{-1}s^{-1}$). The patterned polymer lines are 25 μm wide and 50 μm high. Only the first ~1 cm from the inlet of the capillaries were filled, and it took 30 min or longer to fill the entirety of a 2 cm long capillary (not shown). Filling was not always complete. Although capillaries with larger dimensions (>50 μm, width) took less time to fill (5–10 min), the rate of movement of capillary front slowed considerably after the first ~1 cm.

In contrast, when vacuum (10 torr) was used to pull the liquid polymer into the capillaries, the same pattern could be filled in 15 s (Fig. 2B); larger capillaries filled in a few seconds. Figure 2 suggests that, for conventional MIMIC, the filling of long capillaries slowed significantly after ~1 cm. The time (t) to fill a channel of given width (a), height (b), and length (l) with a liquid with viscosity of η is given by Equation 1. Here, C_g is a geometric term containing width (a) and height (b), and Δp is the drop in pressure.

$$t = \eta l^2 / 2\Delta p C_g \quad (1)$$

Although longer capillaries can be filled more rapidly by vacuum-assisted MIMIC than by MIMIC without vacuum, experiments with long capillaries (>5 cm) showed that the rate of filling also slowed substantially after 2–3 cm for vacuum-assisted MIMIC. We wished to determine the length of capillary that could be filled within a reasonable time (less than 1 min) by vacuum-MIMIC, and to verify that capillary filling still followed the relationship described in Equation 1.

Figure 3a shows the plot of time vs. the length of capillary filled for 25 μm high capillaries having widths of 25, 50, and 100 μm with vacuum-assisted MIMIC. The design of the pattern used for this set of experiment consisted of an array of 5 cm long capillaries that were connected to a single inlet and a single outlet. Initially, for all three capillary sizes, the time varies as the square of the distance of the capillary that is being filled following the relationship

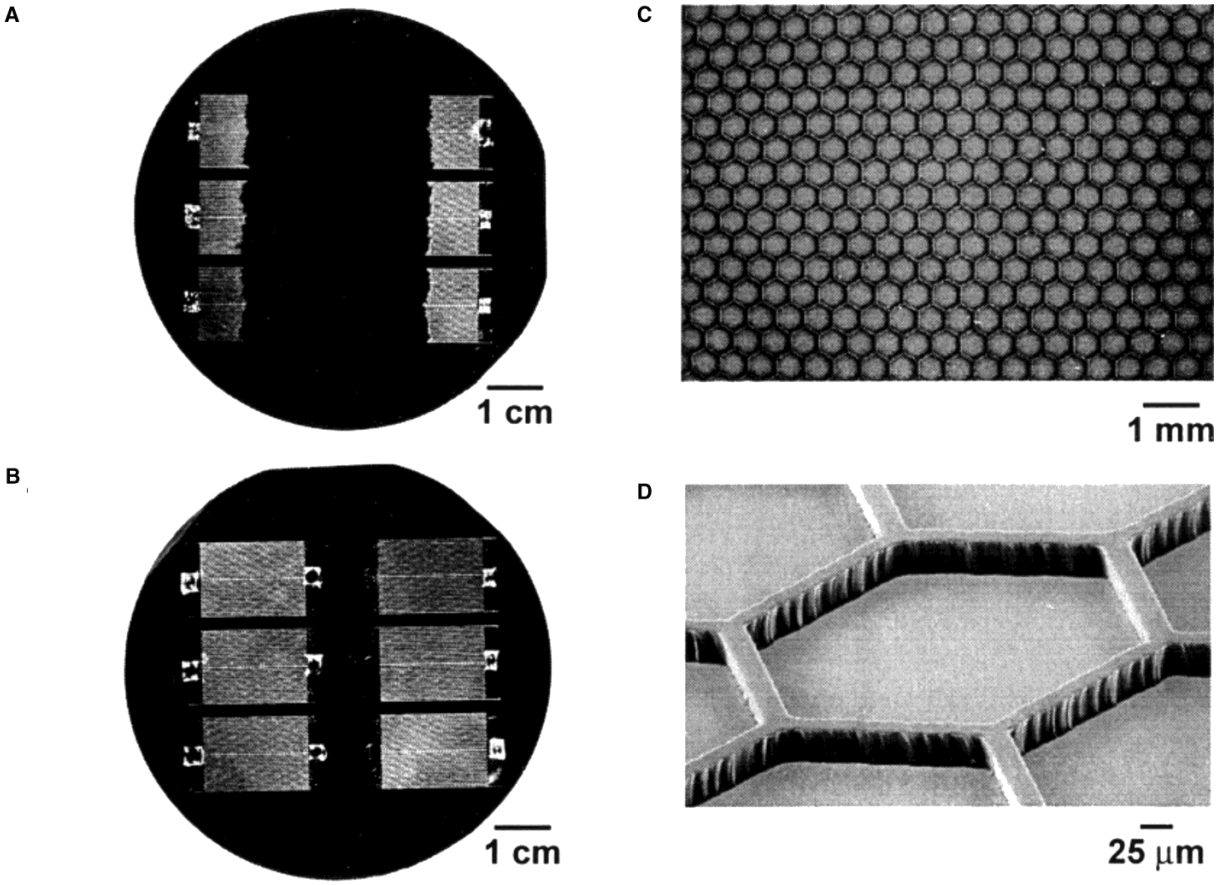

Fig. 2. A) Photograph of a 3 inch wafer partially patterned by MIMIC without vacuum for 15 min. The patterned lines are 25 μm wide and 50 μm high. B) Photograph of the same pattern filled by vacuum-assisted MIMIC in 15 s. C) A higher magnification scanning electron microscopy (SEM) image of the hexagonal design and 25 μm wide polymer patterns shown in B. D) An oblique view SEM of a single hexagonal cell showing high aspect ratio. Structures with aspect ratios of 1:4 have also been fabricated. Note the absence of a polymer underlayer between the patterned hexagonal structures. The features on the sides of these structures were present in the mold, and were generated in the photolithographic process used to make this mold; they are not artifacts of the vacuum-assisted MIMIC process.

0935-9648/99/1108-0948 $ 17.50+.50/0

ADVANCED MATERIALS

shown earlier in Equation 1 (solid lines in Fig. 3). After some distance (with values that were different for different capillary sizes, longer for larger capillaries), the curves deviate from the equation, the rate of filling rapidly slows and the movement of liquids eventually stops. We have not established the origins of the deviations between the observed behavior and the behavior predicted from Equation 1 at time >100 s, for 25 × 25 μm capillaries (Fig. 3a) but they have the consequence of effectively halting flow (at about 4 cm, for this system). Thus, for 25 μm capillaries, it seems that the inlet and the outlet bracketing capillary bed cannot be separated by more than 2–3 cm. For larger capillaries with 50 and 100 μm widths, the filling behavior follows Equation 1 for the entire 5 cm distance and the decrease in flow rate is less significant than for 25 μm wide capillaries. For comparison, Figure 3b shows the plot of time vs. the length of capillary filled by MIMIC for 100 × 50 μm capillary with MIMIC without vacuum. We used considerably larger capillaries since capillaries with sizes shown in Figure 3a were filled extremely slowly, and filling stopped after 5–10 mm.

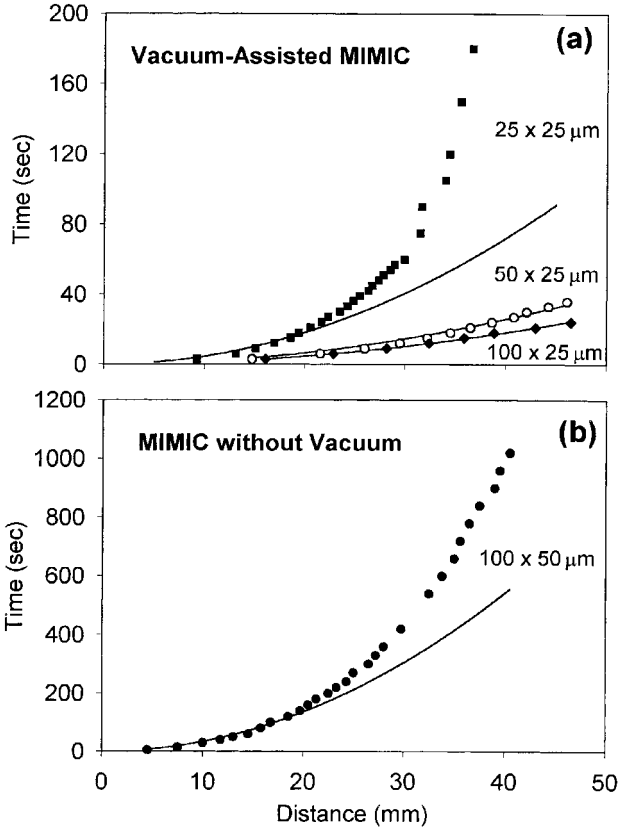

Fig. 3. Graphs of time vs. distance filled for capillaries that were filled by a) vacuum-assisted MIMIC and b) conventional MIMIC without vacuum.

Figure 4 shows additively patterned conducting polymer (polypyrrole-coated polyurethane, DSM, The Netherlands) on a flexible polyimide sheet by vacuum-assisted MIMIC. The conducting polymer was available as a dispersion (20 wt.-%) in water. This polymer dispersion could not be used with conventional MIMIC because of poor wetting of the polyimide, and hence poor performance in capillary filling. The capillaries were filled efficiently, however, when vacuum was used. The polyimide substrates were cleaned by oxidation in O_2 plasma, rinsed with water and ethanol, and dried with nitrogen gas. After the liquid dispersion had completely filled the channels, the sample was placed in an oven to remove the solvent (60 °C). The size of the features that were patterned ranged from 25 μm to larger values. The conductivity of the polymers patterned by vacuum-assisted MIMIC was 0.1 S/cm. This value is similar to that of conventionally prepared films by spin coating or dip coating from this material.

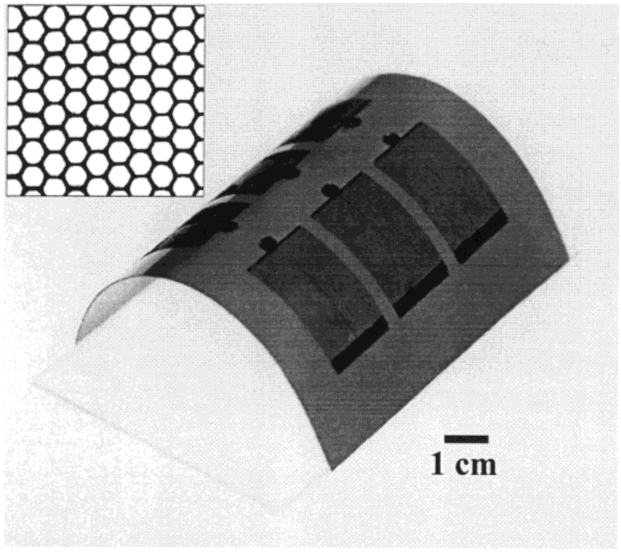

Fig. 4. Photograph of patterned polypyrrole on a flexible polyimide substrate by vacuum-assisted MIMIC. The inset is a high resolution picture showing the quality of the pattern. The polymer was patterned on a flat sheet and bent before taking the photograph.

In summary, this work demonstrated that vacuum-assisted MIMIC—a variation of MIMIC—can be used for rapid patterning of materials over a large area. Compared to conventional MIMIC, smaller and longer capillaries can be filled rapidly and the procedure minimizes or eliminates the underlayer between the features of the pattern that often accompanies MIMIC. The minimum size of features that can be patterned with vacuum-assisted MIMIC depends strongly on the length of the capillary and the viscosity of the fluid; Equation 1 and Figure 3 suggest general guidelines for selecting these parameters.

Vacuum-assisted MIMIC can be used for applications where large area patterning of functional electronic polymers (both conducting and insulating) on flexible and curved substrates is needed. This economical and simple process brings MIMIC closer to practical applications in fabrication of flexible, all organic microelectronic and optoelectronic devices.

Received: February 8, 1999
Final version: April 19, 1999

  0935-9648/99/1108-0949 $ 17.50+.50/0

[1] E. Kim, Y. Xia, G. M. Whitesides, *Nature* **1995**, *376*, 581.
[2] E. Kim, Y. Xia, G. M. Whitesides, *J. Am. Chem. Soc.* **1996**, *118*, 5722.
[3] Y. Xia, G. M. Whitesides, *Angew. Chem. Int. Ed.* **1998**, *37*, 550.
[4] S. Brittain, K. Paul, X. Zhao, G. M. Whitesides, *Phys. World* **1998**, *11*, 31.
[5] F. Garnier, R. Hajlaoui, A. Yassar, P. Srivastava, *Science* **1994**, *265*, 1684.
[6] C. J. Drury, C. M. J. Mutsaers, C. M. Hart, M. Matters, D. M. de Leeuw, *Appl. Phys. Lett.* **1998**, *73*, 108.
[7] A. Dodabalapur, Z. Bao, A. Makhija, J. G. Laquindanum, V. R. Raju, Y. Feng, H. E. Katz, J. Rogers, *Appl. Phys. Lett.* **1998**, *73*, 142.
[8] H. Sirringhaus, N. Tessler, R. H. Friend, *Science* **1998**, *280*, 1741.
[9] H. E. Katz, *J. Mater. Chem.* **1997**, *7*, 369.
[10] A. R. Brown, A. Pomp, C. M. Hart, D. M. de Leeuw, *Science* **1995**, *270*, 972.
[11] A. J. Lovinger, L. J. Rothberg, *J. Mater. Res.* **1996**, *11*, 1581.
[12] Z. Bao, A. Dodabalapur, A. J. Lovinger, *Appl. Phys. Lett.* **1996**, *69*, 4108.
[13] P. E. Burrows, S. R. Forrest, M. E. Thompson, *Curr. Opin. Solid State Mater. Sci.* **1997**, *2*, 236.
[14] D. Bradley, *Curr. Opin. Solid State Mater. Sci.* **1996**, *1*, 789.
[15] Y. Yang, *MRS Bull.* **1997**, *30*, 31.
[16] Z. Bao, Y. Feng, A. Dodabalapur, V. R. Raju, A. J. Lovinger, *Chem. Mater.* **1997**, *9*, 1299.
[17] J. A. Rogers, Z. Bao, V. R. Raju, *Appl. Phys. Lett.* **1998**, *72*, 2716.
[18] W. S. Beh, I. T. Kim, D. Qin, Y. Xia, G. M. Whitesides, *Adv. Mater.*, in press.
[19] J. A. Rogers, Z. Bao, L. Dhar, *Appl. Phys. Lett.* **1998**, *73*, 294.
[20] D. C. Duffy, R. J. Jackman, K. M. Vaeth, K. F. Jensen, G. M. Whitesides, *Adv. Mater.* **1999**, *11*, 546.
[21] E. Kim, Y. Xia, X.-M. Zhao, G. M. Whitesides, *Adv. Mater.* **1997**, *9*, 651.
[22] N. L. Jeon, J. Hu, G. M. Whitesides, M. K. Erhardt, R. G. Nuzzo, *Adv. Mater.* **1998**, *10*, 1466.
[23] J. Hu, R. G. Beck, T. Deng, R. M. Westervelt, K. D. Maranowski, A. C. Gossard, G. M. Whitesides, *Appl. Phys. Lett.* **1997**, *71*, 2020.
[24] J. Hu, R. G. Beck, R. M. Westervelt, G. M. Whitesides, *Adv. Mater.* **1998**, *10*, 574.
[25] T. Deng, L. B. Goetting, J. Hu, G. M. Whitesides, *Sens. Actuators A* **1999**, *75*, 60.
[26] J. A. Rogers, K. E. Paul, G. M. Whitesides, *J. Vac. Sci. Technol. B* **1998**, *16*, 88.
[27] E. Delamarche, A. Bernard, H. Schmid, A. Bietsch, B. Michel, H. Biebuyck, *J. Am. Chem. Soc.* **1998**, *120*, 500.

Magnetic Core–Shell Particles: Preparation of Magnetite Multilayers on Polymer Latex Microspheres**

By *Frank Caruso*,* *Andrei S. Susha*, *Michael Giersig*, and *Helmuth Möhwald*

There is currently immense interest in the fabrication of core–shell particles with unique and tailored properties for various applications in materials science.[1–10] The properties of the core particle can be significantly altered by the shell surrounding the core, whilst the surface properties of such composite particles are governed by the characteristics of the shell. Colloidal particles with magnetic properties have become increasingly important both technologically and for fundamental studies due to the tunable anisotropic interaction they exhibit.[11,12] For example, composite magnetic core–shell particles combine the properties of the individual magnetic particles and non-magnetic sphere dispersions: in the absence of an applied magnetic field the particles have an isotropic sphere dispersion, whereas in an external magnetic field the particles form anisotropic structures.[8]

Composite colloidal particles, for example polymeric or inorganic cores coated with inorganic materials, are commonly fabricated either by direct surface reactions or by controlled surface precipitation of the coating materials on the core.[1–8] More recently, an alternative approach based on the alternate assembly of oppositely charged macromolecular species onto colloidal templates has been employed to fabricate composite core–shell particles.[9,10,13,14] This technique permits the step-wise adsorption of various components as the layer growth is governed by their electrostatic attraction, and allows the formation of multilayer shells with nanometer (thickness) precision. Shells comprising multilayers of various polyelectrolytes have been assembled on colloidal core particles,[14] as have multilayers of inorganic–polymer composites,[9,10,13] where the inorganic materials are zirconium phosphate sheets, silica or alumina nanoparticles. Proteins have also been incorporated in a multilayer shell configuration surrounding colloidal particles using the step-wise electrostatic assembly approach.[15] The potential use of these particles includes separations, affinity chromatography, catalysis and composites.

Herein we report on the production of composite magnetic core-shell particles, where the shell consists of magnetite (Fe_3O_4) nanoparticle/polyelectrolyte multilayers and the colloidal core is polystyrene (PS) latex. Magnetite nanoparticles of average diameter 10–15 nm are alternately deposited with either poly(diallyldimethylammonium chloride) (PDADMAC) or poly(allylamine hydrochloride) (PAH) on the 640 nm diameter PS latices. The influence of an external magnetic field to order the composite PS-core magnetic-shell particles prepared is also investigated. The introduction of a magnetic function to polymer latex colloids provides particles which may be of importance in various technologies (e.g., separations).

Multilayer shells of Fe_3O_4 and polyelectrolyte (PDADMAC or PAH) were prepared on the PS latices pre-coated with a precursor three layer polyelectrolyte film:[9] the outermost layer is PDADMAC or PAH, therefore providing a positively charged surface for Fe_3O_4 deposition. Alternate depositions of Fe_3O_4 and PAH or PDADMAC on the pre-coated PS latices, under conditions where the nanoparticles and polyelectrolyte are oppositely charged (pH ~ 5–6), produce magnetic nanoparticle/polyelectrolyte multilayer

[*] Dr. F. Caruso, A. S. Susha,[+] Prof. H. Möhwald
Max Planck Institute of Colloids and Interfaces
D-14424 Potsdam (Germany)
Dr. M. Giersig
Hahn-Meitner-Institute
Glienicker Strasse 100
D-14109 Berlin-Wannsee (Germany)
[+] Permanent address: Physico-Chemical Research Institute
Belarusian State University, Leningradskaya 14
Minsk, 220080 (Belarus)

[**] A.S. gratefully acknowledges financial support of this work from the Deutsche Forschungsgemeinschaft, Sonderforschungsbereich 1623 and Max-Planck-Gesellschaft, Institut für Kolloid- und Grenzflächenforschung. We thank Norbert Buske from Mediport Kardiotechnik, Berlin, Germany for supplying the magnetite nanoparticles.

  0935-9648/99/1108-0950 $ 17.50+.50/0